CHEMISTRY OF MATERIALS
Article

Chem. Mater. **2011,** *23,* 989–999 989
DOI:10.1021/cm102743y

Quantum Clusters in Cavities: Trapped Au_{15} in Cyclodextrins

Edakkattuparambil Sidharth Shibu and Thalappil Pradeep*

DST Unit on Nanoscience (DST UNS), Department of Chemistry and Sophisticated Analytical Instrument Facility, Indian Institute of Technology, Madras, Chennai 600 036, India

Received September 24, 2010. Revised Manuscript Received December 13, 2010

We have prepared Au_{15} quantum clusters anchored to α-, β-, and γ-cyclodextrin (CD) cavities. The synthesis process involves the core etching of larger clusters and the simultaneous trapping of the clusters formed inside the CD cavities. The clusters were characterized by various tools, such as optical absorption and luminescence spectroscopies, electrospray ionization−mass spectrometry (ESI-MS), X-ray photoelectron spectroscopy (XPS), circular dichroism spectroscopy, and two-dimensional nuclear magnetic resonance (2D NMR) spectroscopy. Trapping of the cluster in the CD cavity was proven by circular dichroism and also by rotational Overhauser effect spectroscopy (ROESY), in terms of the distinct cross peak between proton "e" of the glutathione (−SG) ligand and the "H_3" proton of CD. Dynamic light scattering (DLS) studies showed a hydrodynamic diameter of ∼3−4 nm, indicating one CD molecule per cluster with an extension of one water of hydration. The clusters are intensely luminescent, with major lifetime components of 28, 71, and 24 ps for Au_{15}@αCD, Au_{15}@βCD, and Au_{15}@γCD, respectively. The clusters also are strongly luminescent in the solid state. Both in the solution and in the solid state, the luminescence is sensitive to solvents/vapors. The clusters adhere to glass plates, and the solvent dependency of luminescence was used to create patterns that are erased upon gradual evaporation of the solvent. This self-erasing property was further demonstrated with clusters supported on a thin layer chromatography (TLC) plate. Selective detection of metal ions using the luminescence of the clusters is reported. Evaporation of the cluster solutions leads to luminescent gel-like materials.

Introduction

Quantum clusters (QCs) of gold and silver are new types of materials that are composed of very few atoms, with core sizes in the subnanometer regime, which exhibit several novel properties.[1] These include photoluminescence (PL),[2−4] ferromagnetism,[5] optical chirality,[6] catalysis,[7] etc. Compared to metal nanoparticles, they do not have a continuous density of states, but they are characterized by discrete electronic energy levels. QCs act as a bridge between atomic and nanoparticle behaviors and therefore exhibit properties different from both of these size regimes. They show well-defined absorption features and each cluster, with a specific nuclearity, is distinctly different from the neighboring clusters and, therefore, optical absorption spectra provide an easy way to identify them. QCs exhibit strong PL, and their emission can be tuned from the near-infrared (NIR) region to ultraviolet (UV) by decreasing the core size. In contrast, metallic nanoparticles 2−3 nm in diameter exhibit very weak luminescence with quantum yields[8] in the range of 10^{-4}−10^{-5}, which is, in fact, extremely high, compared to that of bulk gold (10^{-10}).[8] However, QCs exhibit luminescence that is orders of magnitude brighter, with quantum yields in the range of 10^{-1}−10^{-3}.[8]

Among the well-studied gold clusters are those protected with glutathione (GSH), synthesized by reducing Au^{3+} ions in the presence of GSH and separated by polyacryl amide gel electrophoresis (PAGE).[8,9] Chemical compositions of these clusters were identified by electrospray ionization−mass spectrometry (ESI-MS). Among the various QCs, $Au_{25}SG_{18}$ (−SG, glutathione thiolate) is the most thermodynamically stable, with a quantum yield of 1×10^{-3}. The crystal structure of the Au_{25} core with another ligand, $-SC_2H_4Ph$, was solved recently.[10] Among the various monolayer-protected Au_n QCs, Au_{25} was studied extensively by various groups, because of its high stability.[8,11−15] Bigger clusters ($n > 25$) can be converted

*E-mail: pradeep@iitm.ac.in.

(1) Jin, R. Nanoscale **2010**, *2*, 343.
(2) Bigioni, T. P.; Whetten, R. L.; Dag, Ö. *J. Phys. Chem. B* **2000**, *104*, 6983.
(3) Huang, T.; Murray, R. W. *J. Phys. Chem. B* **2001**, *105*, 12498.
(4) Peyser, L. A.; Vinson, A. E.; Bartko, A. P.; Dickson, R. M. *Science* **2001**, *291*, 103.
(5) Crespo, P.; Litran, R.; Rojas, T. C.; Multigner, M.; de la Fuente, J. M.; Sanchez-Lopez, J. C.; Garcia, M. A.; Hernando, A.; Penades, S.; Fernandez, A. *Phys. Rev. Lett.* **2004**, *93*, 087204.
(6) Schaaff, T. G.; Whetten, R. L. *J. Phys. Chem. B* **2000**, *104*, 2630.
(7) Zhu, Y.; Qian, H.; Drake, B. A.; Jin, R. *Angew. Chem., Int. Ed.* **2010**, *49*, 1295.
(8) Negishi, Y.; Nobusada, K.; Tsukuda, T. *J. Am. Chem. Soc.* **2005**, *127*, 5261.
(9) Schaaff, T. G.; Knight, G.; Shafigullin, M. N.; Borkman, R. F.; Whetten, R. L. *J. Phys. Chem. B* **1998**, *102*, 10643.
(10) Zhu, M.; Aikens, C. M.; Hollander, F. J.; Schatz, G. C.; Jin, R. *J. Am. Chem. Soc.* **2008**, *130*, 5883.
(11) Shichibu, Y.; Negishi, Y.; Tsunoyama, H.; Kanehara, M.; Teranishi, T.; Tsukuda, T. *Small* **2007**, *3*, 835.
(12) Shibu, E. S.; Muhammed, M, A, H.; Tsukuda, T.; Pradeep, T. *J. Phys. Chem. C* **2008**, *112*, 12168.

© 2011 American Chemical Society
Published on Web 01/13/2011

to $Au_{25}SG_{18}$ by adding excess GSH under appropriate conditions.[11−13] The most important property of such clusters that is useful for applications is luminescence, and examples along this direction include micropatterning,[14] cell imaging,[15−17] metal ion sensing,[15] and amino acid detection.[18] QCs with chiral protecting monolayers have been reported recently.[19] Applications of QCs as materials require larger quantities of samples, and methods for the rapid synthesis of some of them, such as Au_{25}, are now available.[11,14,15] Despite these efforts, only limited studies exist on other monolayer-protected gold QCs, such as Au_8,[20] Au_{20},[21] Au_{22},[14] Au_{23},[15] Au_{24},[22] etc. No reports exist on the direct synthesis of Au_{15}.

Another approach for making clusters is through the use of cavities. Gold clusters made inside poly(amidoamine) (PAMAM) dendrimer cavities show very high quantum yields (0.1−0.7).[23−25] Au_{25} clusters also were reportedly synthesized inside bovine serum albumin (BSA) cavities.[26] Native lactoferrin has been used to create intensely luminescent gold clusters.[27] Folic acid conjugated Au-BSA QCs were used for molecular-receptor-targeted imaging of folate receptor−positive oral carcinoma cells.[17] Proteins have also been used as etching agents to create clusters.[18] Atomic and electronic structure of gold QCs have been reviewed recently.[28] Highly water-soluble gold clusters with *N*-acetyl-L-cysteine and tiopronin were also reported.[29] However, reports of QCs with other metals have been limited. There have been several recent efforts on silver,[30−33] and some of these QCs show observable luminescence.[30,33] Red-emitting silver clusters (Ag_9) were made via a solid-state route recently.[34]

Scheme 1. Schematic Illustration of Cyclodextrin (CD)-Assisted One-Pot Synthesis of Light-Emitting Gold Quantum Clusters (QCs) via the Core Etching Reaction

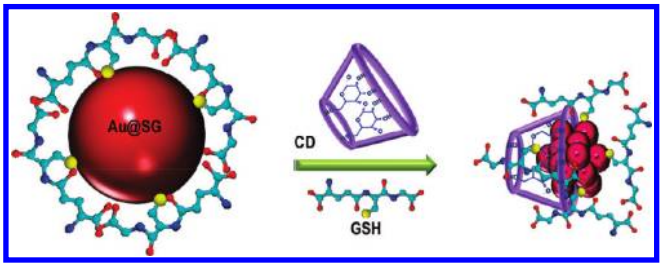

Here, we combine host−guest chemistry with core etching to make QCs in high yield. While larger clusters are etched by ligands to yield smaller clusters, the product formed is trapped in host cavities, to protect it from further core reduction. We have stabilized Au_{15} in cyclodextrin (αCD βCD, and γCD) cavities via this approach. Core etching with excess GSH alone results in Au_{25} clusters protected with GSH.[11,12] The new clusters were characterized by UV−vis, steady-state luminescence, X-ray photoelectron spectroscopy (XPS), electrospray ionization−mass spectroscopy (ESI-MS), two-dimensional hydrogen-ion nuclear magnetic resonance (2D ^{1}H NMR), and circular dichroism studies. Luminescence from the clusters is highly solvent-dependent, which has been used to write patterns on a cluster-coated thin layer chromatography (TLC) plate made of silica. The patterns are self-erasing, and the surfaces can be regenerated repeatedly. The luminescence from the clusters blue shifts by 100 nm by adding of Cu^{2+} ions in ppm concentrations. Scheme 1 shows a cartoon representation of Au_{15} cluster formed inside the CD cavity. Although the Au_{15} core is protected with glutathione, and the entire entity interacts with CD; for the sake of simplicity, we designate the cluster as Au_{15}@CD.

Experimental Section

Materials. All the chemicals were commercially available and used without further purification. $HAuCl_4 \cdot 3H_2O$, methanol (GR grade), ethanol (GR grade), and reduced GSH (γ-Glu-Cys-Gly, molecular weight of 307) were purchased from SRL Chemical Co. Ltd., India. $NaBH_4$ (>90%) was purchased from Sigma−Aldrich. Deionized (DI) water with a resistivity of > 18 MΩ cm^{-1} was used for all the experiments. α-, β-, and γ-cyclodextrins (CD) were purchased from Wako Chemicals, Japan.

Synthesis of Au@SG. Au@SG nanoparticles were synthesized using the reported protocol, with a few modifications.[8] To a 50 mL methanolic solution (0.5 mM) of $HAuCl_4 \cdot 3H_2O$ was added 1.0 mM GSH (1:2 molar ratio, the total volume of methanol was 50 mL). The mixture was cooled to 0 °C in an ice bath for 30 min. An aqueous solution of $NaBH_4$ (0.2 M, 12.5 mL), cooled to 0 °C, was injected rapidly into the above

(13) Muhammed, M. A. H.; Shaw, A. K.; Pal, S. K.; Pradeep, T. *J. Phys. Chem C* **2008**, *112*, 14324.
(14) Shibu, E. S.; Radha., B.; Verma, P. K.; Bhyrappa, P.; Kulkarni, G. U.; Pal, S. K.; Pradeep, T. *ACS Appl. Mater. Interfaces* **2009**, *1*, 2199.
(15) Muhammed, M. A. H.; Verma, P. K.; Pal, S. K.; Arun Kumar, R.; Paul, C. S.; Omkumar, R. Y.; Pradeep, T. *Chem.—Eur. J.* **2009**, *15*, 10110.
(16) Lin, C.-A. J.; Yang, T.-y.; Lee, C.-H.; Huang, S. H.; Sperling, R. A.; Zanella, M.; Li, J . K.; Shen, J.-L.; Wang, H.-H.; Yeh, H.-I.; Parak, H.; Chang, W. H. *ACS Nano* **2009**, *3*, 395.
(17) Archana, R.; Sonali, R.; Deepthy, M.; Prasanth, R.; Muhammed, M. A. H.; Pradeep, T.; Shantikumar, N.; Manzoor, K. *Nanotechnology* **2010**, *21*, 055103.
(18) Muhammed, M. A. H.; Verma, P. K.; Pal., S. K.; Archana, R.; Shantikumar, N.; Manzoor, K.; Pradeep, T. *Chem.—Eur. J.* **2010**, *16*, 10103.
(19) Yao, H.; Miki, K.; Nishida, N.; Sasaki, A.; Kimura, K. *J. Am. Chem. Soc.* **2005**, *127*, 15536.
(20) Muhammed, M. A. H.; Ramesh, S.; Sinha, S. S.; Pal, S. K.; Pradeep, T. *Nano Res.* **2008**, *1*, 333.
(21) Zhu, M.; Qian, H.; Jin, R. *J. Am. Chem. Soc.* **2009**, *131*, 7220.
(22) Zhu, M.; Qian, H.; Jin, R. *J. Phys. Chem. Lett.* **2010**, *1*, 1003.
(23) Zheng, J.; Petty, J. T.; Dickson, R. M. *J. Am. Chem. Soc.* **2003**, *125*, 7780.
(24) Zheng, J.; Nicovich, P. R.; Dickson, R. M. *Annu. Rev. Phys. Chem.* **2007**, *58*, 409.
(25) Zheng, J.; Zhang, C. W.; Dickson, R. M. *Phys. Rev. Lett.* **2004**, *93*, 077402.
(26) Xie, J.; Zheng, Y.; Ying, J. Y. *J. Am. Chem. Soc.* **2009**, *131*, 888.
(27) Xavier, P. L.; Chaudhari, K.; Verma, P. K.; Pal, S. K.; Pradeep, T. *Nanoscale* **2010** *2*, 2769 (DOI:10.1039/C0NR00377H).
(28) Häkkinen, H. *Chem. Soc. Rev.* **2008**, *37*, 1847.
(29) Choi, M. M. F.; Douglas, A. D.; Murray, R. W. *Anal. Chem.* **2006**, *78*, 2779.
(30) Mrudula, K. V.; Udaya Bhaskara Rao, T.; Pradeep, T. *J. Mater. Chem.* **2009**, *19*, 4335.
(31) Diez, I.; Pusa, M.; Kulmala, S.; Jiang, S.; Walther, A.; Goldmann, A. S.; Muller, A. H. E.; Ikkala, O.; Ras, R. H. A. *Angew. Chem., Int. Ed.* **2009**, *48*, 2122.
(32) Wu, Z.; Lanni, E.; Chen, W.; Bier, M. E.; Ly, D.; Jin, R. *J. Am. Chem. Soc.* **2009**, *131*, 16672.
(33) Rao, U. B.; Pradeep, T. *Angew. Chem., Int. Ed.* **2010**, *49*, 3925.
(34) Rao, U. B.; Nataraju, B.; Pradeep, T. *J. Am. Chem. Soc.* **2010**, *132*, 16304.

mixture, under vigorous stirring. The mixture was allowed to react for another hour. The resulting precipitate was collected and washed repeatedly with methanol through centrifugal precipitation. Finally, the Au@SG precipitate was dried and collected as a dark brown powder. The size of Au@SG particles made here is in the range of 2−3 nm.

Cyclodextrin-Assisted Synthesis of Au_{15} Clusters. The above nanoparticles (50 mg) were dissolved in 40 mL of DI water that contained 1.6 mol of GSH and 2.2×10^{-4} mol of cyclodextrin (the three CD molecules were used separately). In this synthesis, GSH is used in excess, because it is an etchant. The CD concentration is ~10 000 times lower than the GSH concentration. A large excess of GSH is typically used in similar core-etching protocols.[12] The mixture was heated at 70 °C for 48 h. The clusters do not form at lower temperatures, and the products decompose at higher temperatures. The completion of the reaction was monitored by checking the red emission of the cluster under UV light. Intense red emission from the sample indicates the formation of the desired cluster. The entire solution was centrifuged at 5000 rpm for 10 min. The whitish-brown precipitate of Au(1)thiolate was discarded. The supernatant was transferred to a plastic vial (to avoid the coating on the surface of the glass vial; see later discussion) and the solution was freeze-dried to obtain a brown powder with intense red emission in the solid state. The same method was used for all three CD molecules, resulting in three separate cluster products. The material was washed twice with ethanol to remove excess GSH. In the synthetic protocol that we have used, the presence of excess CD molecules posed a limitation for CHNS elemental analysis. As the material decomposes during polyacrylamide gel electrophoresis (PAGE), this procedure could not be used to remove excess CD. Nevertheless, examination was performed using energy-dispersive analysis of X-rays (EDAX). The sample becomes a gel if the solution is allowed to dry in air (see later discussion).

Methods. UV−vis spectra were recorded using a Perkin−Elmer Lambda 25 spectrophotometer. To amplify less-intense absorption features, the data have been corrected with the Jacobian factor. For this, the experimentally obtained intensities in absorbance, as a function of wavelength [$I(W)$], have been converted to energy-dependent values [$I(E)$], using the expression

$$I(E) = \frac{I(W)}{\partial E/\partial W} \propto I(W) \times W^2$$

where $\partial E/\partial W$ represents the Jacobian factor. The photoexcitation and luminescence studies were performed using a NanoLog Horiba Jobin-Yvon spectrofluorimeter with a 100-W xenon lamp as the excitation source, at a scan speed of 240 nm/s. The band pass for both excitation and emission monochromators was kept at 5 nm. Metal ion detection was studied at ppm concentrations. Acetates (Cu^{2+} and Hg^{2+}), nitrates (Ag^{1+}, Cd^{2+}, and Zn^{2+}), and chlorides (Fe^{3+}) were used for metal ion detection studies. XPS measurements were done using an Omicron Nanotechnology spectrometer with polychromatic Al Kα X-rays ($h\nu$ = 1486.6 eV). At least 10 spectra in the desired binding energy range were collected and an average was taken. The samples were spotted as drop-cast films on the sample stub and dried under vacuum. The X-ray flux was adjusted to reduce beam-induced damage of the sample. The energy resolution of the spectrometer was set at 1.1 eV, at a pass energy of 50 eV. The binding energy (BE) was calibrated with respect to C 1s at 285.0 eV. Luminescence transients were measured and fitted using a commercially available spectrometer (Lifespec-ps) from Edinburgh Instruments, U.K. (with an instrument response function (IRF) of 80 ps). ^{1}H NMR and 2D ^{1}H NMR (ROESY) spectra were measured with a 500 MHz Bruker Advance III spectrometer operating at 500.13 MHz for ^{1}H NMR and was equipped with a 5-mm triple-resonance PFG probe. Solutions were made in 99.98% D_2O (Aldrich) and sealed immediately. The signal of the solvent served as the reference for the field-frequency lock. All experiments were performed at a temperature of 25 °C, unless specified. Standard Bruker pulse programs (Topspin 2.1) were employed throughout. The 1D spectra were acquired with 32K data points. The data for phase-sensitive ROESY experiments were acquired with a sweep width of 5600 Hz in both dimensions. For each spectrum, 16 transients of 2048 complex points were accumulated for 256 t_1-increments and a relaxation delay of 2 s was used. A continuous-wave (CW) spin-lock mixing time of 200 ms was employed. Prior to Fourier transformation, zero filling to 2K × 2K complex points was performed, and apodized with a weighted function (QSINE) in both dimensions. All the data were processed on a HP workstation, using Topspin 2.1 software. Mass spectrometric studies were conducted using an electrospray (ESI-MS) system (Applied Biosystems, Model 3200 Q-TRAP LC/MS/MS). Samples with a concentration of 15 ppm, taken in a 1:1 water/methanol mixture, were electrosprayed at a flow rate of 10 μL/min and an ion spray voltage of 5 kV. Circular dichroism studies were measured using a Jasco Model J-810 circular dichroism spectropolarimeter. The limit of detection (LOD) of GSH in circular dichroism is ~0.1 mg/mL. The optical polarization image was measured using a Nikon Model Eclipse LV100 POL polarizing microscope. DLS measurements were made with a Nano-S Malvern instrument, employing a 4 mW He−Ne laser (λ = 632.8 nm) equipped with a thermostatted sample chamber. All the scattered photons are collected at a scattering angle of 173°. The scattering intensity data are processed using the instrumental software to obtain the hydrodynamic diameter (d_h) and the size distribution of the scatterer in each sample. The instrument measures the time-dependent fluctuation in the intensity of light scattered from the particles in solution at a fixed scattering angle. The hydrodynamic diameter (d_h) is estimated from the intensity autocorrelation function of the time-dependent fluctuation in intensity; d_h is defined as

$$d_h = \frac{k_B T}{3\pi\eta D} \quad (1)$$

where k_B is the Boltzmann constant, η the viscosity, and D the translational diffusion coefficient. In a typical size distribution graph from the DLS measurement, the x-axis shows the distribution of size classes (in nanometers), while the y-axis shows the relative intensity of the scattered light. This is therefore known as an intensity distribution graph. Several standard samples have been studied.

Results and Discussion

Quantum clusters (QCs) show well-defined absorption features, which are distinctly different from those of the neighboring clusters. Figure 1A shows the UV−vis spectra (Jacobian-corrected) of all three clusters in water (see the Experimental Section for the synthesis method). All three clusters (with various CDs) have characteristic absorption features at 318, 458, and 580 nm, where there are no features for GSH as well as CD. All the CDs are optically transparent in the 200−1100 nm window. Pure GSH has an absorption in the 200−250 nm window. The absorption profile of pure GSH and CD are given in

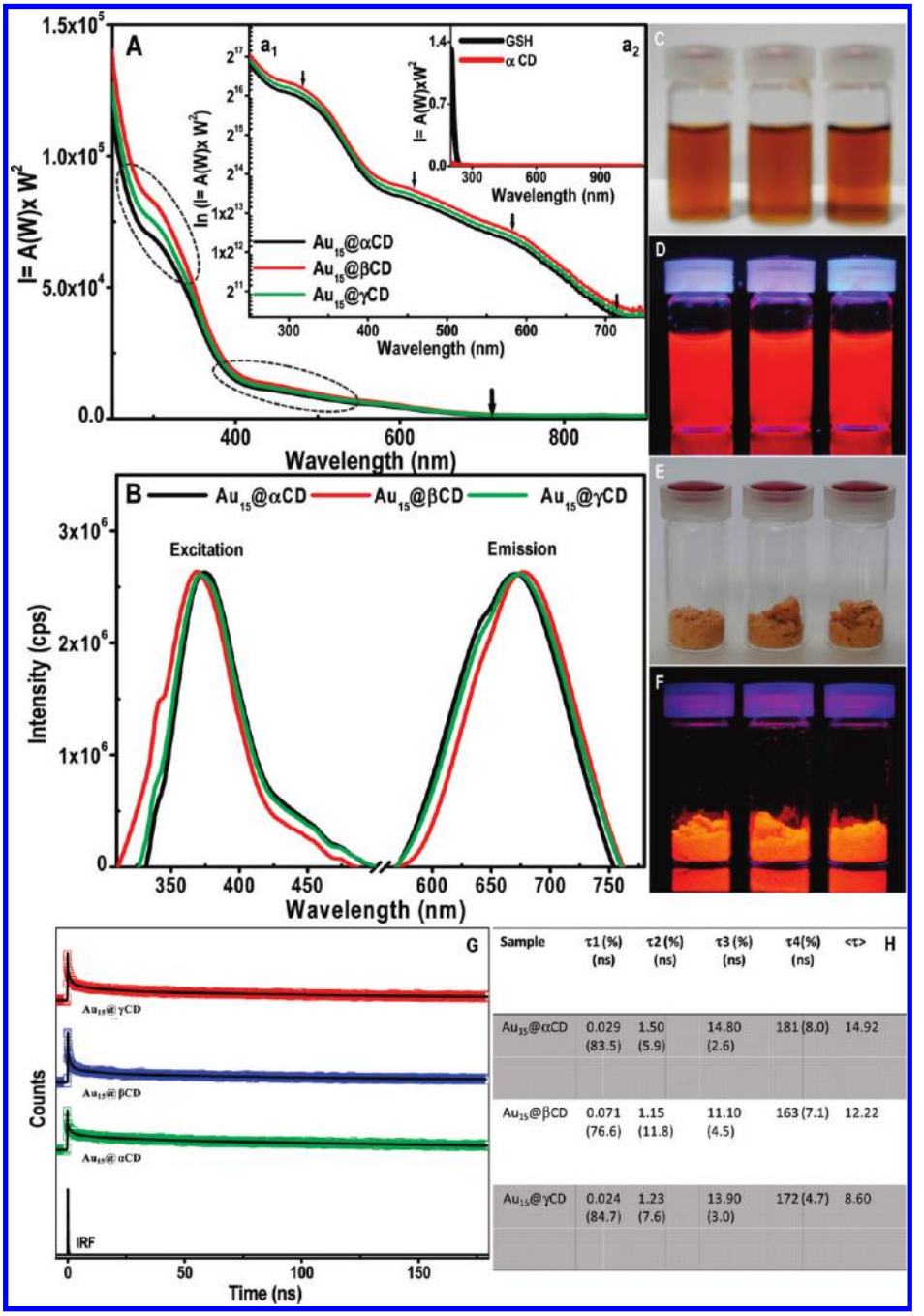

Figure 1. (A) UV−vis spectra of Au_{15}@αCD, Au_{15}@βCD, and Au_{15}@γCD clusters inside the CD cavity. Ellipses indicate the distinct features of the Au_{15} core. Inset a_1 gives the plot of the natural logarithm of the Jacobian factor, versus wavelength, of all three clusters, to show the molecular features more clearly. Well-defined absorption features are marked with arrows. The threshold of absorption is also marked. Absorption profiles of pure GSH and αCD are given in inset a_2. (B) PL spectra of all three samples (375 nm excitation). (C) Photograph of the cluster solutions under white light. (D) Photograph of the cluster solutions under UV light. (E) Photograph of the three cluster powders under white light. (F) Photograph of the three cluster powders under UV light. (G) Luminescence decay of Au_{15}@αCD, Au_{15}@βCD, and Au_{15}@γCD clusters in water. (H) Table giving the lifetime values for Au_{15}αCD, $Au_{15}\beta$CD, and $Au_{15}\gamma$CD.

inset (a_2) in Figure 1A. The cluster features are better manifested in a semilogarithmic plot, shown in inset (a_1) in Figure 1A. This absorption feature resembles the molecule-like absorption of $Au_{15}SG_{13}$, which has been reported.[8] The same core reduction reaction performed with 1−2 nm Au@SG particles (prepared with a Au:GSH ratio of 1:4) and in the absence of CD results in $Au_{25}SG_{18}$, which is the most stable cluster in this group,[8] as known from several studies.[11−13] The formation of Au_{25} clusters in such a core reduction process without CD has been studied using time-dependent UV−vis spectroscopy. The appearance of a peak at 672 nm (characteristic intraband transition of the Au_{25} core) confirms the formation of Au_{25} clusters (see Figure S1 in Supporting Information-I), apart from the well-defined other features, which are characteristic of the cluster. In cases such as Au_{25}, where spectral features are distinct, absorption spectrum alone is enough to characterize the clusters formed. In the CD-assisted method, we do not see this characteristic profile and we do see any peak at 672 nm, which confirms that the new clusters are

entirely different from Au_{25}. The well-defined absorption features are marked with arrows in the inset. The threshold of optical absorption indicates a band gap of 1.75 eV. These characteristic signatures[8] confirm that the cluster formed is Au_{15}. The fact that the absorption threshold occurs at a lower wavelength than those of Au_{25}, Au_{22}, and Au_{18} points to a smaller core than Au_{18}. Moreover, the threshold is located at a higher wavelength than that of Au_{10}, implying a larger core than itself. The only core observed in the window (below Au_{18} and above Au_{10}) is Au_{15} for the Au−GSH system,[8] which further supports the assignment of Au_{15}. The synthetic conditions used (the Au:S ratio, the presence of CD) and the stabilizing nature of CD cavities may be responsible for the formation of Au_{15}, under these conditions. We have compared the UV−vis spectra of Au_{15} clusters with other GSH-protected gold clusters that have been reported from our group. The optical features of this newly formed cluster is entirely different from others (Au_{31},[15] Au_{25},[12] Au_{23},[15] and Au_{22}[14]), which excludes all other possibilities. Data given in Figure S2 in Supporting Information-I show a systematic trend in the threshold of optical absorption.

We have studied the formation of Au_{15}@CD using the time-dependent UV−vis spectroscopy. The interesting observation in this study is that, when Au@SG is undergoing core reduction in the presence of GSH and CD, initially, Au_{25} is formed (within 3 h). This is clearly shown by the intraband transition of Au_{25} at 672 nm. However, as time progresses, the Au_{25} core decomposes and new optical absorption features of Au_{15} appear. This clearly suggests that the so-called core reduction of Au@SG with CD and GSH follows the Au_{25} route. The formation of Au_{15}@CD could be due to the extra stability of the system inside the CD cavity. The time-dependent UV−vis data are given in Figure S3 in Supporting Information-I.

The optical absorption features of Au_{15}@CD are not sharp, unlike those observed in the case of QCs such as Au_{25}, Au_{22}, and Au_{23}. This could be because the QC is partially inside the cavity. The QCs formed inside the PAMAM cavity do not show sharp optical absorption features, which has been reported in several cases.[23−26] A recent example is protein encapsulated clusters.[17,18,27]

The luminescence spectra (Figure 1B) of the three clusters show a NIR emission, with a maximum of 690 nm (at 375 nm excitation). Although there is an apparently large Stokes shift, the excitation tails to a much-longer wavelength window. This is typical in many systems, such as Au_{22},[14] Au_{23},[15] Au_{10},[8] etc. This is also a characteristic of the Au_{15} core.[8] The images shown in Figures 1C and 1D show photographs of the cluster solutions under white light and UV light, respectively. The clusters also show intense emission in the solid state. Solid-state emission has been an interesting subject area in materials chemistry for the past few years for various reasons. The images shown in Figures 1 E and 1F show photographs of the cluster (α, β, and γ) powders under white light and UV light, with intense emission. The photographs under white light and UV light are taken under different ambiences and, therefore, the two sets of images do not overlap. The luminescence decays of all three clusters (in water) were measured using a picosecond-resolved, time-correlated, single-photon-counting (TCSPC) technique. The decay profiles of these clusters (at 375 nm excitation) are given in Figure 1G. Lifetime values of the clusters were obtained by numerical fitting of the luminescence at 690 nm (Figure 1H). They are 0.029 ns (83.50%), 1.50 ns (5.90%), 14.80 ns (2.60%), and 181 ns (8.0%) for Au_{15}@αCD; 0.071 ns (76.6%), 1.15 ns (11.8%), 11.10 ns (4.5%), and 163 ns (7.1%) for Au_{15}@βCD; and 0.024 ns (84.7%), 1.23 ns (7.6%), 13.90 ns (3.0%), and 172 ns (4.7%) for Au_{15}@γCD. The fast lifetime component is present in several of the clusters investigated so far, which also shows an extremely slow component with reduced weight. For example, the Au_{22} system shows a fast lifetime component of 0.05 ns (86.50%) and a slow component of 141.80 ns (3.40%).[14] The quantum yields of the clusters are ~6.7% (Au_{15}@αCD), 6.5% (Au_{15}@βCD) and 7.0% (Au_{15}@γCD) at room temperature, using ethidium bromide (EtBr) as the reference. In comparison to other similar systems, this value is substantially larger. Examples include Au_{22} (4%)[14] and Au_{23} (1.3%).[15] The PL spectra of these QCs show a large Stokes shift. The exact reason for the shift in these QCs is not known in the literature. However, one possible reason could be the energy cascade within the sp-derived excited states, facilitated by the concomitant energy relaxation through structural distortion and low-energy excitation of the ligands.

Isolated clusters are not seen clearly via transmission electron microscopy (TEM), although nanoparticles are observed before the etching reaction. As in the case of the Au_{25} core,[12] the clusters aggregate under exposure to an electron beam.[12] The core size of these clusters is in the range of 0.5−0.7 nm. The cyclodextrin (CD) molecules are known to form self-assembled microstructures. Hence, we could see only cluster-embedded CD self-assembly. The QCs aggregate under exposure to an electron beam. The effect of electron-beam exposure can be minimized by reducing the accelerating voltage of the electron beam. To reduce the beam-induced damage, TEM images were taken at 100 kV and the data are given in Figure S4 in Supporting Information-I. The nature of the core in these clusters was confirmed by XPS analysis. The photoelectron spectra of all three samples in the Au 4f region are given in Figure S5 in Supporting Information-I. The $4f_{7/2}$ and $4f_{5/2}$ BE values of gold in all these clusters appear at 85.2 and 89.2 eV, respectively, which match with the data reported for Au_{15}.[8] Measurable shifts in the BE values are observed for differently sized clusters.[8,12−15] The S 2p, N 1s, and C 1s core level spectra of these clusters were also measured, and the data are given in Figure S5 in Supporting Information-I, which are all consistent with the molecular nature of the cluster. The Au/S atomic ratio measured from XPS is 1.150, which is consistent with a composition of $Au_{15}S_{13}$ (the theoretical value is 1.1538). The reported Au_{15} core has 13 −SG ligands.[8] The S $2p_{3/2}$ BE value at 162 eV is characteristic of thiolate. This is observed in clusters and also in self-assembled monolayers on gold. The free thiol value is in the range of 164 eV. The

GSH protection is intact, which is clear from the presence of the S 2p and N 1s positions. The N 1s spectrum shows two peaks at BE values of 399.5 and 401.3 eV, indicating the presence of $-NH$ and $-NH_3^+$, respectively. The C 1s and N 1s of the samples show minor differences, because these are due to the outer protection, namely, monolayers and CD. Even in these, the qualitative features are the same; however, in these, the distinct components have different weights. These changes are expected in such materials; reasons could be different extents of surface contamination and changes due to X-ray exposure.

We studied the negative-ion ESI-MS of Au_{15}@αCD in detail (in 50:50 water:methanol). The mass range available in QTrap 3200 is not enough to see the singly charged cluster. Besides, orthogonal ESI-MS does not give intact cluster species.[8] Hence, we could not see the intact Au_{15} core. However, we see the presence of CD, −SG, and small fragments of the QCs. The peaks at m/z 972, 995, and 1150 are assigned to CD^-, $CD+Na^-$ and $CD_2-SG+2Na^-$, respectively. The cluster fragment observed is at m/z 1418, and is due to $[Au_3CD_2SG]^{2-}$ with sodium addition, which occur at m/z 11.5 spacing, because it is doubly charged. Data are given in Figure S6 in Supporting Information-I. Matrix-assisted laser desorption ionization mass spectroscopy (MALDI MS), using sinapinnic acid and α-cyano-4-hydroxycinnamic acid (CHCA), did not reveal any cluster features. Trans-2-[3-(4-tert-butylphenyl)-2-methyl-2-propenylidene] malononitrile (DCAB) matrix, which gives a good spectrum[35] for $Au_{25}(SC_2H_4)_{18}$, did not prove successful in this case.

To understand the size of the QCs in solution, we performed DLS measurements (see Figure S7 in Supporting Information-I). The observed hydrodynamic diameter of the clusters is 3−4 nm, which implies the presence of one cluster per CD molecule with one water of hydration. However, the −SG of the cluster, associated with one CD cavity, can also interact with another CD molecule. The wider rim of βCD has a diameter of 15.3 Å,[36] which is adequate for molecular penetration. The largest molecule observed to form an inclusion complex in βCD is 1-adamantanecarboxylic acid, which has a molecular dimension of 7 Å.[36] Although the structure of the Au_{15} core is not available from single-crystal XRD studies, calculations suggest that it has a C_{2v} symmetry, shell-like flat cage structure with a pointed tip.[37] It is possible that some of the core or monolayers can penetrate into the CD cavity (see below). The inner core diameter is in the range of 0.6−0.9 nm for αCD, βCD, and γCD, respectively. This is sufficiently large to partially accommodate Au_{15} clusters. These clusters have a tendency to form gel-like structures at a particular concentration (as discussed later). The broadening seen in DLS may be due to the aggregating tendency of the QCs.

We have confirmed the presence of −SG and CD molecules in the sample, using ^{1}H NMR. ^{1}H NMR of Au_{15}@αCD is shown, along with those of pure GSH and αCD in Figure S8A in Supporting Information-I. The data show the presence of both −SG protection and αCD in the cluster sample. All the peaks are labeled. The features of −SG are the same as those reported earlier.[12,13] ^{1}H NMR of pure GSH shows six characteristic peaks. GSH is a tripeptide that consists of three amino acids, namely, glutamic acid, cysteine, and glycine. The molecular structures of GSH and CD are given in Figure S8B in Supporting Information-I. The peaks at 2.1 ppm (e), 2.4 ppm (d), and 4.5 ppm (f) respectively correspond to the γ $-CH_2$, β $-CH_2$, and α −CH molecules of glutamic acid. Peaks at 2.8 ppm (c) and 3.8 ppm (a) are due to the β $-CH_2$ and α −CH molecules of cysteine. The peak of the α −CH species of glycine occurs at 3.7 ppm (b). In the ^{1}H NMR of the cluster, two sets of protons c, d, and e (marked as c−e and c_I−e_I) are shown. This clearly indicates that −SG molecules sitting on the surface of the cluster are in two different environments; we suggest that one is included in a CD cavity and the other is outside the CD cavity. Both of these are clearly shifted from the parent GSH positions, indicating that there is no free GSH. Of the two sets of protons, one set is more down-shielded, compared to the other, because of the nearest presence of the gold core. This down-shielded proton (proton "e") has a cross peak with the H_3 proton of the CD molecule (see below). The (down-shielded) proton "e" and proton "d" have been shifted in their positions (by 12.1 and 10.2 Hz, respectively). Moreover, proton "c" was broadened (an expanded view of the spectra is given in Figure S8C and S8D in Supporting Information-I). The same features also were observed in β- and γCD clusters.

CD molecules have six characteristic peaks and are labeled as H_1−H_6 (see Figure S8A in Supporting Information-I). In the cluster, the H_3 proton has been shifted. For the other protons, substantial broadening has been observed. Thus, the NMR data affirm that GSH is bound to the Au core in the thiolate form. The UV−vis, XPS, and NMR data, together, support the formation of $Au_{15}SG_{13}$ within CD. With the passage of time, especially for long NMR measurements, it appears that some free GSH is produced, because of its desorption from the cluster surface. These molecules appear as weak features at positions of the parent GSH.

Insight into the incorporation of the cluster inside the CD cavity was provided by 2D ^{1}H NMR (ROESY). The cross peaks in ROESY are indicative of specific proximity relationships between adjacent protons (the distance between protons is generally within 5 Å).[38] A ROESY spectrum of Au_{15}@αCD is given in Figure 2A. Although the spectrum appears complicated and the peaks of the protons of CD and −SG overlap each other, the cross peaks between the inner proton of CD (H_3) and −SG proton (proton "e", marked with circles in Figure 2B) are observable. This clearly indicates that some of the −SG molecules of the Au_{15} clusters are inserted into the CD cavity through the wide rim of the CD molecule, which is

(35) Dass, A.; Srevenson, A.; Dubay, G. R.; Tracy, J. B.; Murray, R. W. *J. Am. Chem. Soc.* **2008**, *130*, 5940.
(36) Taulier, N.; Chalikian, T. V. *J. Phys. Chem. B* **2008**, *112*, 9546.
(37) Bulusu, S.; Zeng, X. C. *J. Chem. Phys.* **2006**, *125*, 154303.
(38) Liu, Y.; Shi, J.; Guo, D.-S. *J. Org. Chem.* **2007**, *72*, 8227.

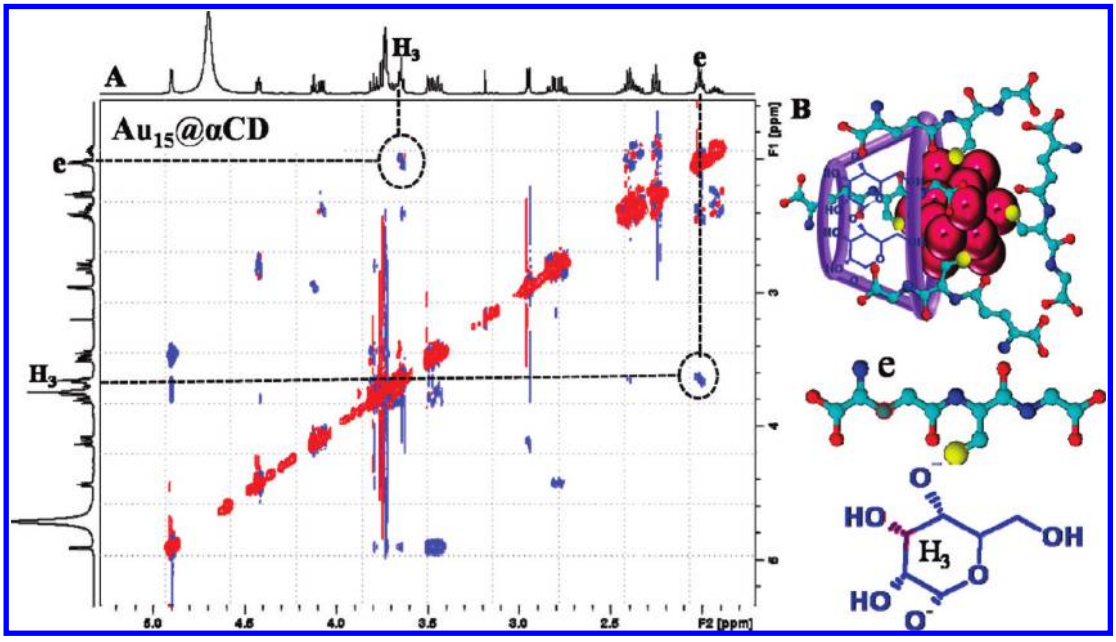

Figure 2. (A) ROESY spectrum of Au_{15}@αCD cluster in D_2O at 25 °C with a mixing time of 200 ms. (B) Schematic illustration showing the possible interaction of proton "e" of the −SG ligand of the cluster with the "H_3" proton of the CD molecule.

shown in the illustrated representation in Figure 2B. For the sake of clarity, we have marked only the relevant peaks in the 2D spectrum. Other details are marked in Figure S8 in Supporting Information-I. Similar ROESY experiments were performed for other two clusters, which also show the same type of cross peak. The data are given in Figure S9 in Supporting Information-I. The shift in the positions of proton "e" (from 2.03 ppm to 2.0 ppm) and of −SG and the "H_3" proton (from 3.9 ppm to 3.7 ppm) of CD, compared to parent molecules, clearly confirm the host−guest interaction. These shifts are clearly marked in Figure S8A in Supporting Information-I.

The CDs used are optically transparent and have no signal in the spectropolarimeter, whereas GSH is chiral, which shows a negative Cotton peak at ~237 nm. Inclusion complexes of CD show induced circular dichroism.[38] The chromophore-appended CDs were used as fluorescence sensors for the recognition of bile salt.[38] Complex formation of pyromellitic diimide derivatives with β-cyclodextrin and anthracene-appended β-cyclodextrin were studied using induced circular dichroism.[39] An anthracene-appended β-cyclodextrin was used for self-assembly and photoinduced electron-transfer processes.[40] Circular dichroism of $Au_{25}SG_{18}$ has been reported recently.[41] The circular dichroism spectrum of a $Au_{25}SG_{18}$ cluster is given in Figure 3, along with spectra for all three CD clusters and pure GSH. There is no negative Cotton signal at 237 nm in the spectrum of the cluster, which clearly indicates that there is no unbound GSH in the cluster. In the spectrum of $Au_{25}SG_{18}$, all the signals are similar to those reported.[41] There is no report on the chirality of Au_{15} clusters. The spectrum of Au_{15} is entirely different

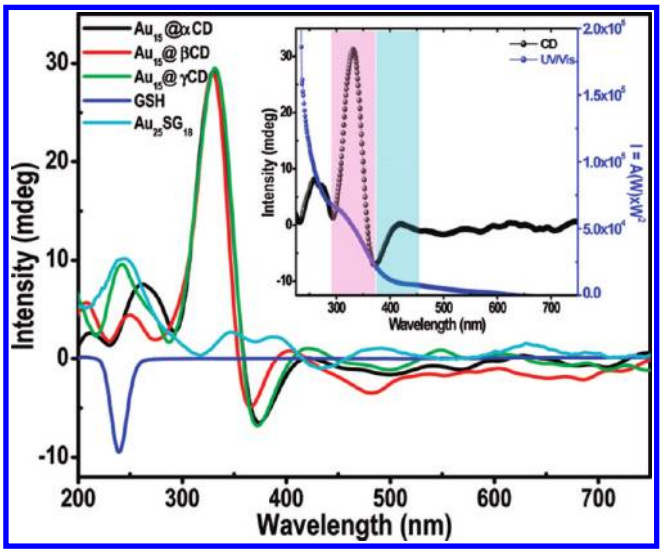

Figure 3. Circular dichroism spectra of Au_{15}@αCD, Au_{15}@βCD Au_{15}@γCD clusters along with pure GSH and $Au_{25}SG_{18}$. The positive Cotton peak at ~330−380 nm and a negative Cotton peak at ~400−455 nm are attributed to the cluster core. Inset shows the combined plot of absorption and CD spectra of Au_{15}@αCD, with one-to-one matching. The UV−vis spectrum (corrected with the Jacobian factor) has been scaled so that the data points of the two measurements match.

from that of pure $Au_{25}SG_{18}$ (position and peak intensity have been changed drastically) and GSH. Thus, the binding of −SG to the Au_{15} core clearly is not the reason for the new spectral features of these clusters. The signal at 330 nm exactly matches with the cluster absorption in the 300−380 nm window, and the second signal at 400−430 nm also matches the 400−455 nm absorption features of the cluster (both of them have been marked). All these information confirm induced circular dichroism in Au_{15}@CD clusters. The 2D NMR and circular dichroism data, together, support the presence of the guest Au_{15} within the CD cavity. In case of Au_{15}@βCD, the signal at

(39) Bijitha, B.; Deepthi, D. L.; Gopidas, K. R. *Org. Lett.* **2007**, *9*, 2709.
(40) Bijitha, B.; Gopidas, K. R. *Chem.—Eur. J.* **2007**, *13*, 5173.
(41) Wu, Z.; Gayathri, C.; Gil, R. R.; Jin, R. *J. Am. Chem. Soc.* **2009**, *131*, 6535.

400−455 nm is slightly different from that of the other two cases. This could be due to solubility and greater hydrophobicity of βCD, which may not accommodate the cluster as well as that observed in the other cases. The size of Au QCs is adequately small to accommodate the cluster inside the CD cavity. The large size of Au nanoparticles limits their incorporation inside the CD cavity.

The storage of these CD-appended Au_{15} clusters in glass bottles for 24 h results in the self-coating of the materials on the inside glass surface. To show this self-coating phenomenon, we have stored Au_{15}@αCD in a 20-mL glass vial for one day and then decanted the solution. The empty glass vial shows a thin layer of the clusters. This layer is not detached, even after sonication for 10 min (in water). The photograph (under white light) of the glass vial with the cluster coating is given in Figure 4A. The same vial under UV light shows an enhanced red emission, as shown in Figure 4B. This clearly indicates that the cluster is intact after self-coating and sonication. We have used the interaction of the cluster and the glass (SiO_2) to paint the material over glass plates. These QCs have a great tendency to form gel-like materials (see more details in Figure 5), which adhere to the surfaces. Interaction of the −OH groups of CD with salinol groups of silica may be responsible for this adhesion. Photographs of the cluster-coated glass plate under white light and UV light are given in Figures 4C and 4D. We extended this phenomenon of cluster−SiO_2 interaction to coat the former on a thin layer chromatography (TLC) plate that has a bulk-SiO_2 coating, as well as nano- and micro-SiO_2 particles. Figures 4E and 4F show photographs of the cluster-coated TLC plate at two different concentrations. At low concentration (Figure 4E), a rose-colored emission is observed; at high concentration (Figure 4F), a red emission is observed. We made luminescent patterns on the TLC plate. One of them is shown in the inset of Figure 4E. Figure 4G shows a confocal luminescence image of the cluster-coated SiO_2 particles (1 μm in diameter, larger concentration). An expanded view of one SiO_2 particle is given in the inset in Figure 4G.

The cluster-coated TLC plate was used as a substrate to examine the solvent dependency of PL. The emission from the cluster-coated TLC plate was collected with 375 nm excitation. Isopropanol then was sprayed over the plate, using a sprayer. Immediately after spraying, emission was collected using the same excitation. Here, we see a slight enhancement of the luminescence intensity. The plate was allowed to dry completely, resulting in the reversal of luminescence. A few other alcohols, such as methanol and ethanol, were sprayed. Luminescence increased in the following order: isopropanol < methanol ≈ ethanol. However, the exposure of water on the TLC plate drastically reduced the luminescence intensity. No shift in the emission wavelength was observed. The emission data are given in Figure 4H. The solvent-dependent emission also was observed in other QCs.[15,29,32,42] The reason for the solvent dependency of emission is attributed to hydrogen bonding of the solvent molecules with ligands on the cluster. As a result, the nonradiative rate of decay is likely to be reduced, which will enhance the emission.[15] Here, the emission of QCs with isopropanol is less, compared to that with methanol and ethanol. The exact reason for this effect is not known. However, a possible reason could the positive inductive effect. As the chain length of the alkyl group increases, the electron density of the −OH molecule will be greater. This will reduce the hydrogen bonding of solvent molecules with the ligands on the QCs. In addition to the cluster emission, we see a peak at 725 nm, which is attributed to the emission from the TLC plate. The solvent dependency of the cluster emission has been used to write letters on the TLC plate. In this approach, the TLC plate is coated with a lower concentration of the cluster so that the emission intensity is weak (and the plate is rose in color). When we write with a solvent, which enhances luminescence intensity, the solvent-exposed regions appear with brighter luminescence. As the solvent evaporates, the parent luminescence reappears, returning the plate to the original state of luminescence. In an experiment, an ethanol-dipped brush was used for writing, because this solvent shows the highest enhancement in luminescence. Photographs were collected using a high-resolution digital camera (see Figure 4I). These letters disappeared as the solvent evaporated from the plate, making them available for fresh writing. The process was repeated several times. We captured a movie of the same experiment, showing the self-erasing properties of the clusters supported on a SiO_2 plate; this is shown in Supporting Information-II. In this movie, one can clearly see the appearance of the letters while writing with ethanol, because of the enhancement in luminescence and the disappearance over time, indicating the evaporation of ethanol.

At higher concentrations, QCs have a tendency to form a gel-like material with intense emission. Self-assembly of the CD and −SG molecules at high concentration may result in gelation. Photographs of the gelated material, under white light and UV light, are shown in Figures 5A and 5B, respectively. This seems to be the first report of a gel using QCs. These materials were analyzed by scanning electron microscopy (SEM) and high-resolution transmission electron microscopy (HRTEM). The microstructure of the gel is composed of fibers ~8 μm in diameter (see inset c_1 in Figure 5C). To study the spatial distribution of gold in the gels formed by QCs, elemental mapping was carried out using an energy-dispersive analysis of X-rays (EDAX). Figure 5C shows the EDAX spectrum collected from the gel shown in inset c_1. EDAX mapping was done using Au Mα irradiation, and the image is given in inset c_2 in Figure 5C. The detailed structure of the fibers was examined by TEM (see inset c_3 in Figure 5C). As previously mentioned, the isolated clusters are not observed via TEM analysis. In both TEM and SEM analyses, we see an elongated fiber-like morphology. CDs and their derivatives have been extensively used as host

(42) Díez, I.; Pusa, M.; Kulmala, S.; Jiang, H.; Walther, A.; Goldmann, A. S.; Muller, A. H. E.; Ikkala, O.; Ras, R. H. A. *Angew. Chem.* **2009**, *121*, 2156.

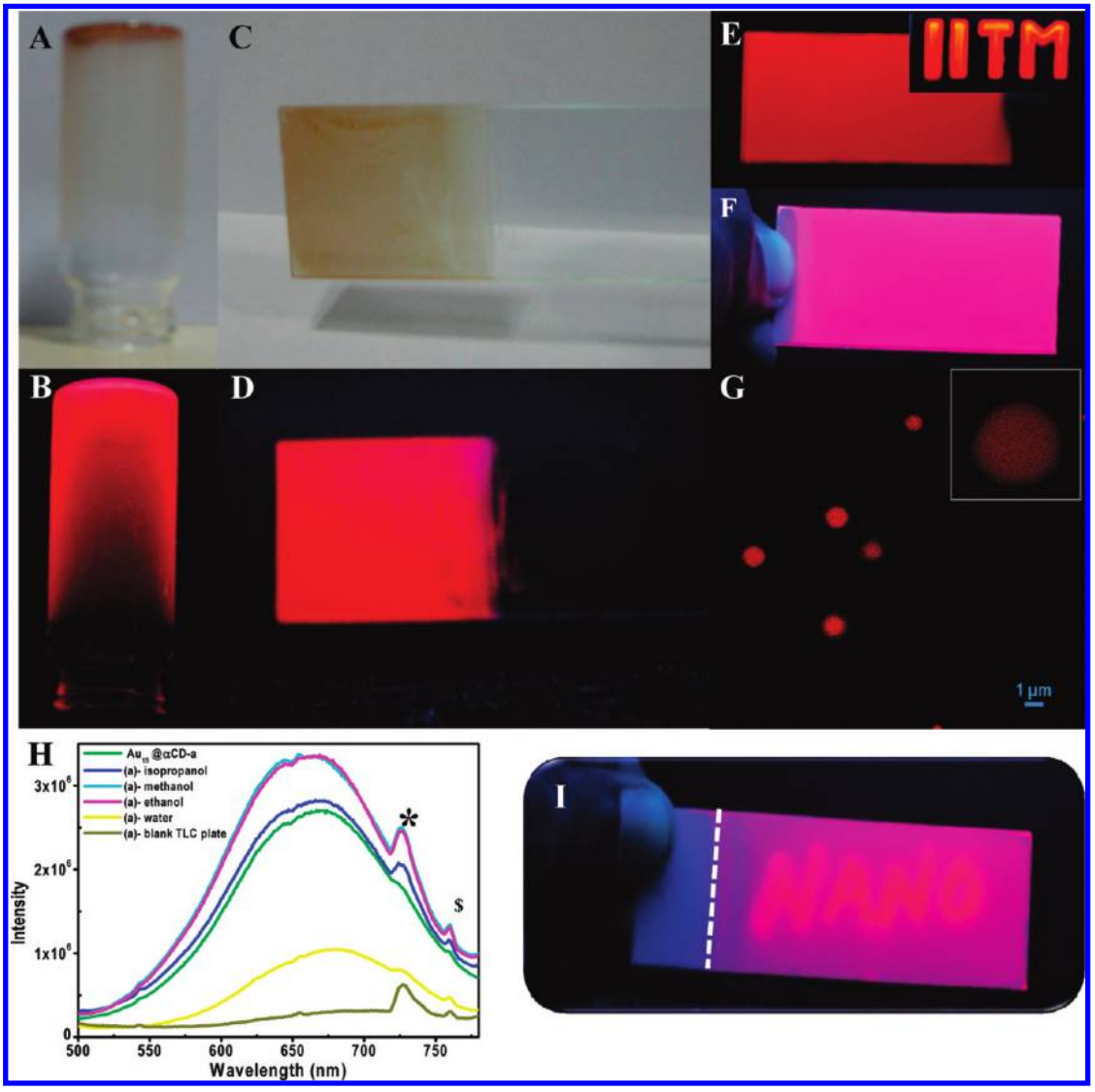

Figure 4. (A) Photograph of the cluster-coated glass vial under white light. (B) Photograph of the cluster-coated glass vial under UV light. (C) Photograph of the cluster-coated glass plate under white light. (D) Photograph of the cluster-coated glass plate under UV light. (E, F) Photographs of the cluster-coated TLC plate at different cluster concentrations (the luminescent pattern "IITM", made in the TLC plate, is also shown in the inset in panel E). (G) Luminescence image of cluster-coated nano-SiO_2 nanoparticles. (Inset in panel G shows a single SiO_2 nanoparticle.) (H) Solvent-dependent PL emission collected from a cluster-coated TLC plate with various solvents. The asterisk symbol (∗) corresponds to regions where a higher-order line of the grating masks the spectrum; the dollar symbol ($) corresponds to the emission coming from SiO_2. (I) Image showing a pattern written over the Au_{15}-coated TLC plate by writing with an ethanol-dipped brush. (The plate was coated with the clusters up to the white line; the blue emission observed closer to the finger in the image is due to the parent TLC plate.)

molecules in supramolecular chemistry. Inclusion complexes (ICs) of CDs and guest molecules may result in supramolecular nanostructures (nanogels). The first report on this was the formation of a "molecular necklace" that is formed due to the inclusion of CD-based polymer ICs.[43,44] The IC between hydrophobic alkyl chains grafted on a polysaccharide (dextran) and poly(CD) polymer resulted in supramolecular spherical nanogels.[45] Similarly, the inclusion of poly(ethylene glycol) (PEG)-modified chitosans and αCD resulted in hydrogels in aqueous media.[46] CDs are known to form ICs with a variety of hydrophobic drug molecules.[47] Such nanoassemblies may find applications in drug delivery and diagnosis, especially in view of the low metallic content of the cluster and its high solubility in water, in conjunction with luminescence. The Au_{15}@CD cluster is soluble only in water. Hence, we used water as a solvent medium to make the cluster solutions.

The mechanism of this type of hydrogel formation is mainly associated with intermolecular hydrogen bonding with the host and guest molecules. In this particular case, water can act as an efficient solvent to make a saturated solution of QCs, as well as a medium for the making gels

(43) Harada, A.; Li, J.; Kamachi, M. *Nature* **1992**, *356*, 325.
(44) Harada, A. *Coord. Chem. Rev.* **1996**, *148*, 115.
(45) Gref, R.; Amiel, C.; Molinard, K.; Daoud-Mahammed, S.; Sébille, B.; Gillet, B.; Claude Beloeil, J.; Ringard, C.; Rosilio, V.; Poupaert, J.; Couvreur, P. *J. Controlled Release* **2006**, *111*, 316.
(46) Huh, K. M.; Cho, Y. W.; Chung, H.; Kwon, I. C.; Jeong, S. Y.; Ooya, T.; Lee, W. K.; Sasaki, S.; Yui, N. *Macromol. Biosci.* **2004**, *4*, 92.
(47) Monza da Silveira, A.; Ponchel, G.; Puisieux, F.; Duchêne, D. *Pharm. Res.* **1998**, *15*, 1051.

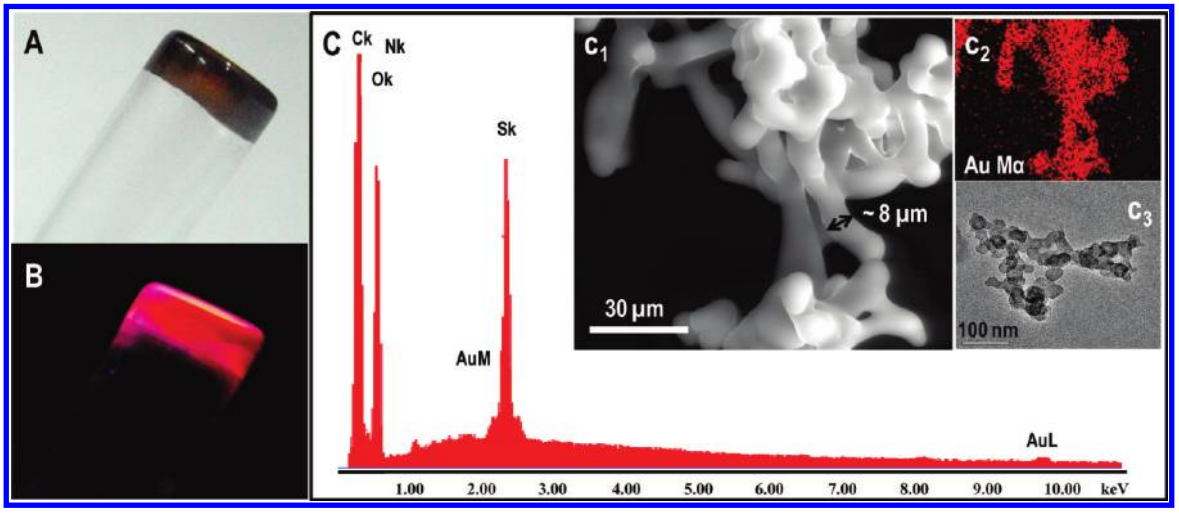

Figure 5. Photographs of the gel formed by QCs in water (A) under white light and (B) under UV light; the inverted bottle illustrates the gel-like appearance. (C) EDAX spectrum of gel formed by QCs (inset c_1 shows the SEM image of a gel formed by QCs; inset c_2 shows EDAX mapping of the gel using Au Mα irradiation, corresponding to the SEM image in inset c_1; and inset c_3 is a TEM image of the gel, showing the self-assembly with a fiberlike morphology.

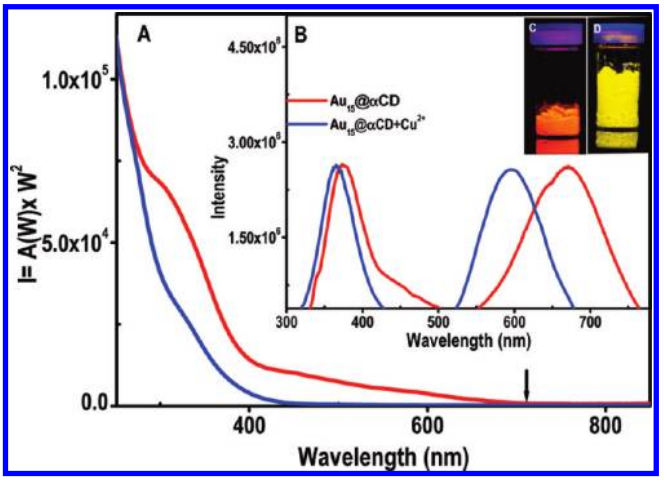

Figure 6. (A) UV−vis spectra and (B) PL spectra of the Au_{15}@αCD cluster before and after the addition of Cu^{2+}. Insets show photographs of the cluster powder under UV light before the addition of Cu^{2+} (inset C) and after the addition of Cu^{2+} (inset D).

via intermolecular hydrogen bonding between the host and guest molecules.

We have utilized the red emission from the clusters for the selective detection of metal ions (Cu^{2+}). We have used different metals ions, such as Fe^{3+}, Zn^{2+}, Ag^{1+}, Cu^{2+}, Cd^{2+}, Hg^{2+}, etc. for the detection experiments. Metal ions were added to aqueous solutions of the QCs (1 mg mL^{-1}), such that their final concentrations were 1 μM, and the emission of the QC was measured immediately after the addition of the ions. In the case of Cu^{2+}, we could see a drastic change, such as the immediate disappearance of the red emission, followed by the emergence of a yellow emission (all these occurred within a few minutes). In the case of Fe^{3+}, PL was quenched immediately. For all other metal ions tested, there was no change in PL. The UV−vis and luminescence spectra of cluster solution before and after the addition of Cu^{2+} are given in Figures 6A and 6B. There is no drastic change in the absorption spectrum of the cluster, even after the addition of Cu^{2+}, because the molecular absorption features are still intact (see Figure 6A), suggesting that the cluster is stable. However, by looking into the PL spectra of the clusters before and after the addition of Cu^{2+}, we can see a drastic change in the maximum emission (a blue shift of ~100 nm). Insets C and D show the photographs of the cluster powder under UV light before and after the addition of Cu^{2+}. The exact reason for the spectral shift after the addition of Cu^{2+} is not known. We have calculated the quantum yield of the QCs after the addition of Cu^{2+}. The quantum yield was slightly decreased (from 6.7% to 5.5%).

Conclusions

We demonstrated the synthesis of an inclusion complex of Au_{15} clusters, formed by the core etching of larger particles and the simultaneous trapping of the product clusters in cyclodextrin cavities. The clusters were characterized by various spectroscopic and microscopic techniques. The host−guest interaction was proved by circular dichroism and two-dimensional nuclear magnetic resonance (2D NMR) spectroscopy. The one-to-one matching of absorption features and circular dichroism peaks indicates the presence of induced circular dichroism. These quantum clusters (QCs) were coated on a bulk SiO_2 plate and SiO_2 particles. Solvent dependency of the cluster emission was used to make a self-erasing platform by coating the cluster over a thin layer chromatography (TLC) plate. The red emission from the cluster has been used for the selective detection of Cu^{2+}. The gelating properties of these QCs in water have been demonstrated. The synthetic methodology presented may be adapted to make a variety of such clusters. Such inclusion complexes of QCs present an interesting new area of nanomaterials, in view of their demonstrated properties.

Acknowledgment. The authors thank the Department of Science and Technology (DST), Government of India, for

constantly supporting our research program on nanomaterials. Thanks are due to P. K. Verma and Dr. S. K. Pal (Satyendra Nath Bose National Centre for Basic Sciences, Kolkata, India) for DLS and lifetime measurements. The authors also thank Dr. A. Ajayaghosh, Dr. K. R. Gopidas, and Mr. K. Retheesh (National Institute of Interdisciplinary and Technology, NIIST), for the circular dichroism measurements. Thanks are due to Dr. C. Baby (SAIF, IIT Madras) for NMR measurements. E.S.S. thanks the University Grants Commission (UGC) for a senior research fellowship.

Supporting Information Available: Supporting Information-I includes time-dependent UV−vis spectra during the core etching reaction of Au@SG nanoparticles with excess GSH (without CD molecules); a comparison of optical features of different −SG-protected gold QCs with Au_{15}; time-dependent UV−vis spectra taken during the core etching reaction of Au@SG QCs with GSH and CD molecules; an HRTEM image of Au_{15}@CD QCs taken at 100 kV; XPS spectra of all the clusters; ESI-MS analysis of Au_{15}@αCD, along with that of pure αCD; DLS analysis of all the clusters in water; ^{1}H NMR analysis of Au_{15}@αCD, along with pure GSH and αCD; and ROESY analysis of Au_{15}@βCD Au_{15}@γCD clusters. (PDF) Supporting Information-II is a video showing the self-erasing properties of the QCs coated on a TLC plate. (AVI) This material is available free of charge via the Internet at http://pubs.acs.org.